Available online at www.sciencedirect.com
SCIENCE DIRECT®
Theoretical and Applied Fracture Mechanics 42 (2004) 139–148
theoretical and applied fracture mechanics
www.elsevier.com/locate/tafmec

Residual stress effect on fatigue striation spacing in a cold-worked rivet hole

P.F.P. de Matos [a,*], P.M.G.P. Moreira [a], J.C.P. Pina [b], A.M. Dias [c], P.M.S.T. de Castro [a]

[a] Department of Mechanical Engineering and Industrial Management, Faculty of Engineering, University of Porto, Rua Dr Roberto Frias, Porto 4200-465, Portugal
[b] Department of Physics, University of Coimbra, 3004-516 Coimbra, Portugal
[c] Department of Mechanical Engineering, University of Coimbra, 3004-516 Coimbra, Portugal

Available online 22 September 2004

Abstract

The residual stress effect due to cold-working is studied in relation to fatigue striation spacing. Cold-working introduces a compressive stress field around the hole reducing the tendency for fatigue cracks to initiate and grow under cyclic mechanical loading. It is known that fatigue lifetime assessment requires a detailed knowledge of the residual stress profile. X-ray diffraction and 3D finite element analysis (FEA) can be used to determine the residual stress profile. Scanning electron microscopy (SEM) measurements were performed for measuring the striation spacing.

Keywords: X-ray diffraction; Residual stress; Finite element analysis; Scanning electron microscopy; Striation spacing

1. Introduction

Problems related with ageing aircraft may be reduced by enhancing the fatigue performance, especially in critical zones, acting as stress raisers, such as access and riveted holes. Fastener hole fatigue strength may be enhanced by creating compressive residual circumferential stresses around the hole. This technique (cold-work) has been used in the aeronautical industry for the past thirty years to delay fatigue damage and retard crack propagation. Research has been concentrated mainly on modelling the residual stress field using analytical or numerical two-dimensional (2D) or three-dimensional (3D) methods [1–5], on the experimental measurement of the residual stress field

* Corresponding author.
E-mail address: pfpmatos@fe.up.pt (P.F.P. de Matos).

0167-8442/$ - see front matter © 2004 Elsevier Ltd. All rights reserved.
doi:10.1016/j.tafmec.2004.08.003

[6,7], on the experimental characterization of the cold-worked hole behaviour in fatigue [8,9], and on the stress intensity factor calibration for cracks that may develop after cold-work [3,10,11]. Sub-topics considered include the consideration of thickness effects [1,12], the consideration of eventual pre-existence of cracks of various sizes before hole expansion is carried out [8], the possible

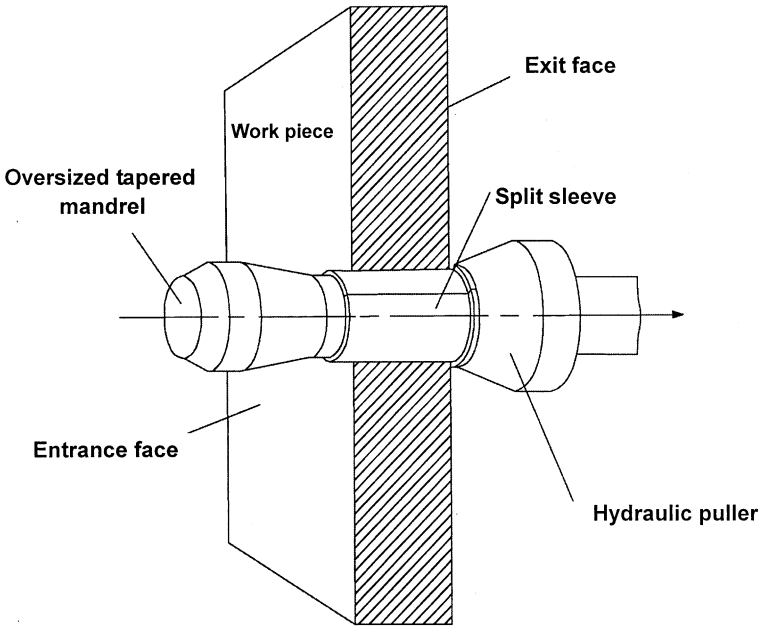

Fig. 1. Schematic diagram of the FTI cold-working process, after Ref. [15].

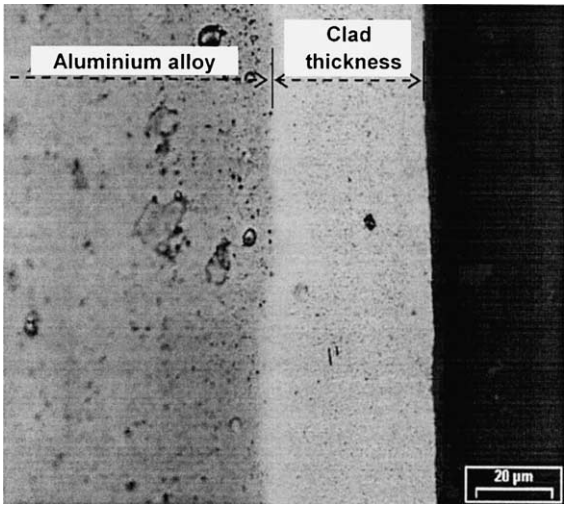

Fig. 2. Metallographic observation of the specimen clad thickness.

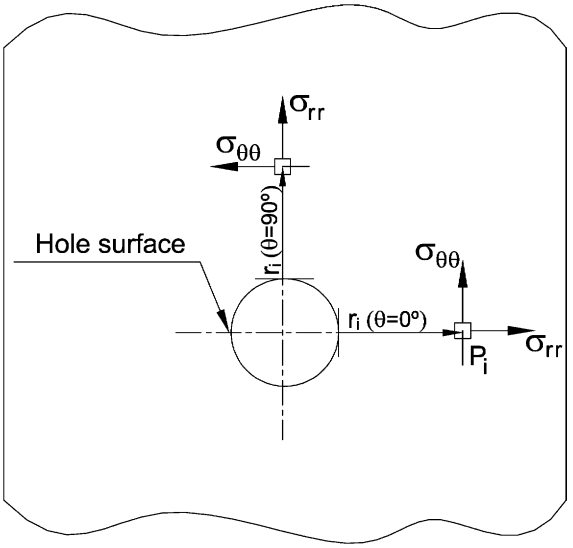

Fig. 3. Radial (σ_{rr}) and circumferential ($\sigma_{\theta\theta}$) stresses for $\theta = 0°$ and $\theta = 90°$.

re-cold-working of already cold-worked holes [13], and the stress analysis of neighbouring cold-worked holes [14,15].

The compressive circumferential residual stress field around the rivet holes is created by applying pressure on the hole surface by means of a mandrel. Once the pressure is removed, the desired residual compressive stress field is achieved. Two cold-working processes are normally used in the aeronautical industry [16,17]: the split sleeve process, using a solid tapered mandrel and a lubricated split sleeve, and the split mandrel process, using a lubricated, hollow and longitudinally slotted tapered mandrel, see Fig. 1.

In what follows, the effect of rivet hole cold-working is investigated in relation to fatigue striation. The material used is aluminium alloy 2024-T3 Alclad. The specimens' geometry is a rectangular plate (280 mm × 25 mm) with a central hole of 4.83 mm diameter. Two specimens one with and other without cold-working were fatigue tested at a constant maximum stress level of 140 MPa, at stress ratio $R = 0.1$ and frequency $f = 10$ Hz in order to study the residual stress effect on the fatigue striation spacing.

2. Analysis by X-ray diffraction

The X-ray diffraction measurements were performed on a 4-circle goniometer, provided with a germanium detector. Cu-Kα radiation was used for all the data collection. In order to have access to the core aluminium without the clad interference, the coating was removed around the periphery of the hole by using electrolytic polishing. The clad thickness was previously measured by microscopic observation, and a mean value of 40 μm was determined for both the faces (see Fig. 2). For this purpose, the hole was fulfilled with an epoxy resin, to avoid the hole wall attack, and the clad was removed by successive layers until a thickness comprised between 35 and 40 μm. This process was controlled by using a micrometer with 1 μm of precision. The phase analysis showed a crystallographic texture that should be considered in the method used for the stress analysis. The ideal directions method was used to collect the data and the calculations were performed by the method suggested in Ref. [18]. The circumferential direction was not an ideal direction of diffraction, thus meaning that the circumferential stress determination was not directly accessible. The problem was solved by the stress tensor calculation, taking the radial as the 11 direction. Each measured point corresponds to the centre of one irradiated rectangle area of $2 \times 1\,\text{mm}^2$ (1 mm in the radial direction). The points were distributed in two directions, as shown in Fig. 3, and on both faces of the specimen, entrance and exit faces. The aluminium (422) reflection was used

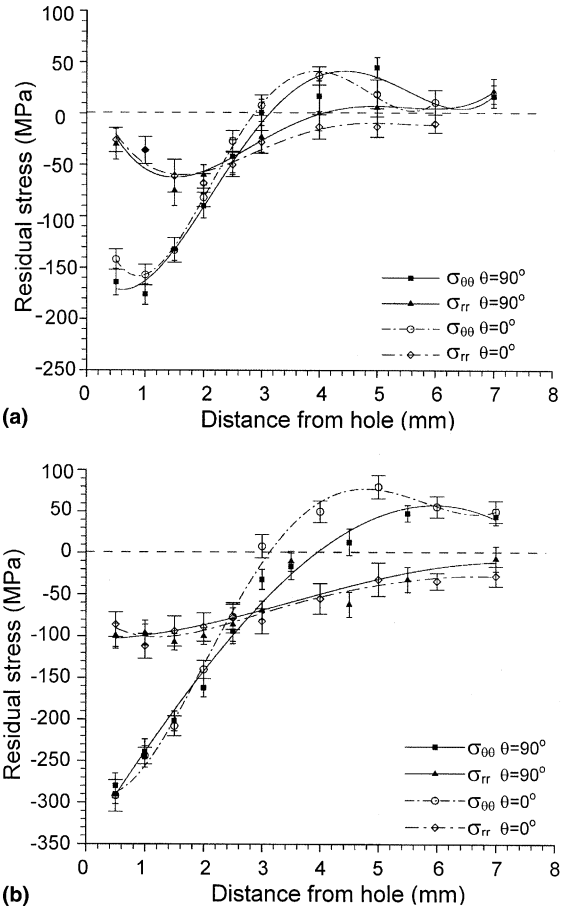

Fig. 4. Residual stresses for $\theta = 0°$ and $\theta = 90°$: (a) entrance face; (b) exit face.

at a diffraction angle of $2\theta = 137.44°$. This means a mean depth penetration of 30 μm for the X-ray radiation.

2.1. X-ray results

The texture analysis on the Al plate showed two components which were identified as the Goss texture $\{110\}\langle001\rangle$ and the cube texture $\{100\}\langle001\rangle$. According to the literature, they are due to the rolling operation and the posterior recrystallization treatment of the plate. The residual stress results are presented in Fig. 4 for both faces referred to in Fig. 1 and the entrance and exit faces of the specimen. A polynomial fitting of the values is also suggested in the figure. Compressive stresses are observed in the vicinity of the hole, with values higher on the exit face than in the entrance face, confirming the through-thickness variation of the stress field.

3. Finite element analysis

Three-dimensional FEA were performed using ABAQUS [19]. Literature reports that the actual method of cold-working where a tapered mandrel is drawn through the hole, gives a variation of the residual stress through the thickness [15,20–22]. 3D finite element analyses were, therefore, carried out: (i) the cold-working process has been simulated accurately by drawing a rigid mandrel through the plate and (ii) a simpler model of hole expansion. The boundary conditions are presented in Fig. 5. Mandrel and sleeve diameter dimensions were taken from FTI [23] catalogue for a hole diameter of 4.83 mm corresponding 4.5% of hole expansion. It must be mentioned that according to FTI [23] for typical fastener hole diameters in aluminium and mild steel, the applied expansion ranges from 3% to 6%. The applied expansion is given by the following formula:

$$i = \frac{(D + 2t - \mathrm{SHD})}{\mathrm{SHD}} 100\% \tag{1}$$

where D is the major mandrel diameter, t is the sleeve thickness and SHD is the starting hole diameter. Frictionless conditions were assumed between the mandrel and sleeve, and the sleeve and the aluminium alloy plate. The assumption of fric-

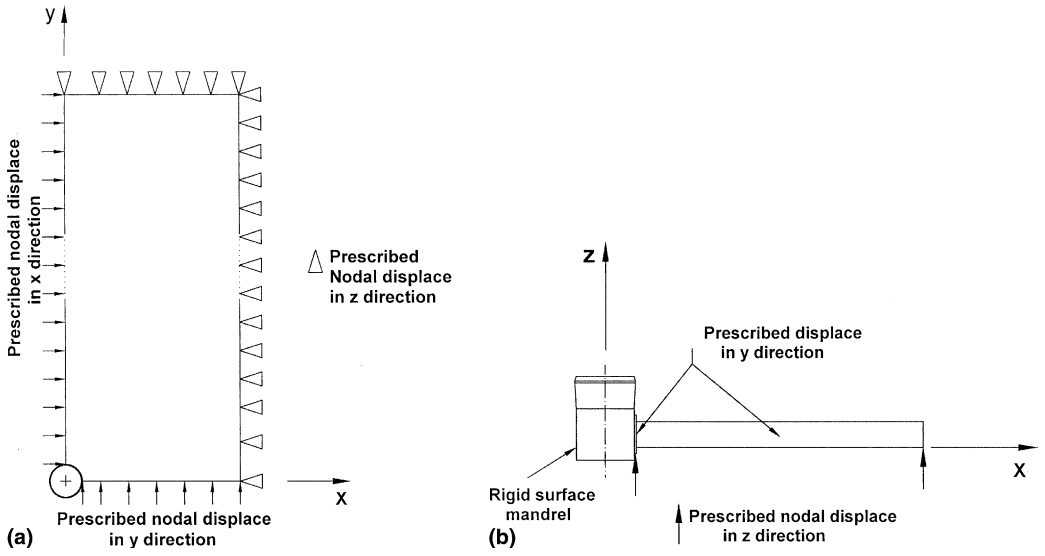

Fig. 5. Finite element model boundary conditions: (a) plane *xy*; (b) plane *xz*.

tionless contact is justified since the sleeve is well defined and slip occurs between the mandrel and sleeve rather than the sleeve and plate.

A linear elastic model was used for the sleeve with a Young's modulus of 210 GPa and Poisson's ratio of 0.3. The mandrel was modelled as a rigid surface, using the revolution feature of ABAQUS. The finite element model has 42,200 three-dimsional eight-node linear elements with eight integration points. The aluminium alloy plate and the steel sleeve were modelled by 41,600 and 600 elements, respectively, (see detail in Fig. 6). The contact between the hole surface and sleeve and also between the sleeve and the mandrel was modelled. Zero friction was assumed between the contacting surfaces. It must be mentioned that sixteen elements along the plate thickness were used.

Initial work and other Ref. [20] showed that considerable refinement of the mesh on the surface of the plate and in the vicinity of the hole edge Fig. 6 is required as also reported in Ref. [15]. In the present work non-linear geometric and material procedures were used.

The material models used are presented in Fig. 7, material elastic perfectly plastic (MEPP) and

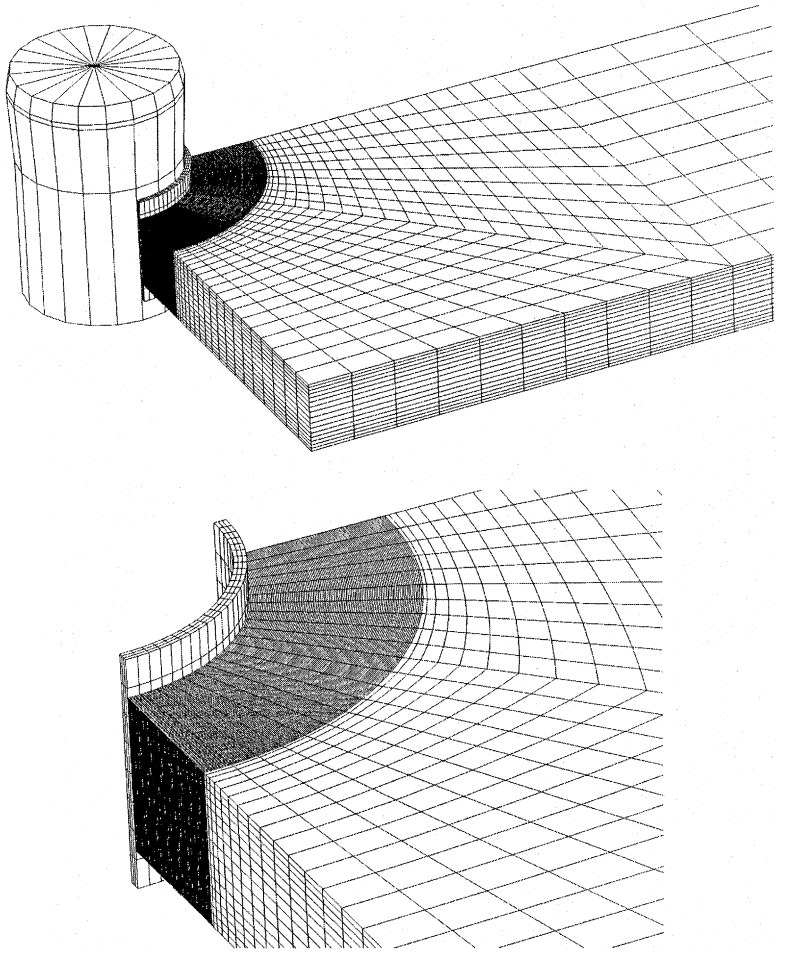

Fig. 6. Model assembly, details.

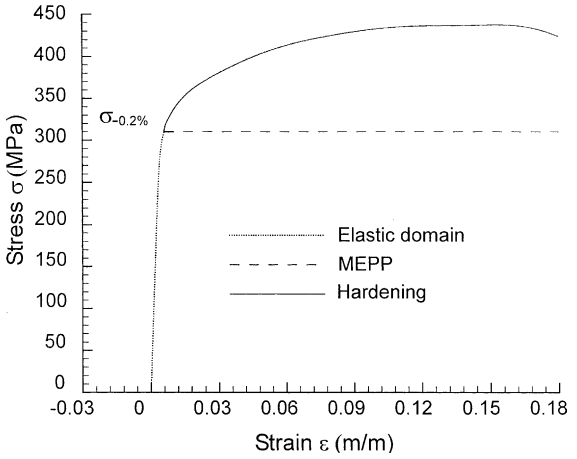

Fig. 7. Material models used in the FEA.

hardening material behaviour. The hardening behaviour was modelled using experimental data points from a tensile test.

4. Comparison of results

Figs. 8 and 9 compares experimental X-ray measurements with FEA results considering an MEPP material model, for $\theta = 0°$. Figs. 10 and 11 compares the experimental X-ray measurements with FEA results considering an hardening material behaviour, for $\theta = 0°$.

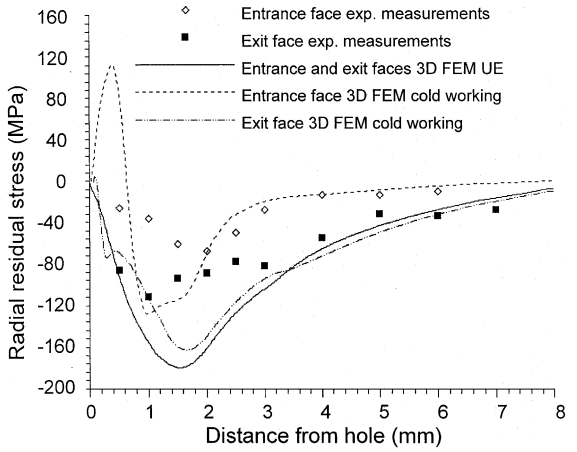

Fig. 8. Radial residual stress, for $\theta = 0°$, MEPP.

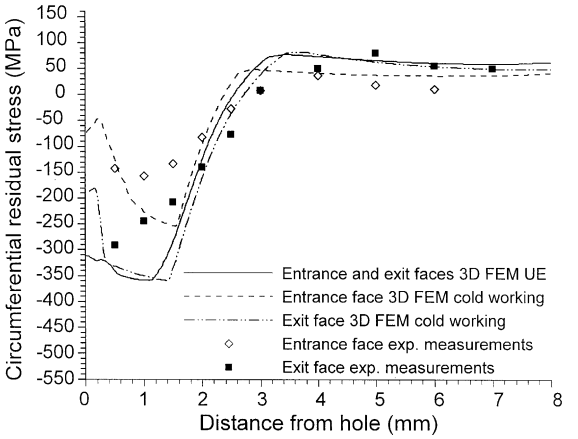

Fig. 9. Circumferential residual stress, for $\theta = 0°$, MEPP.

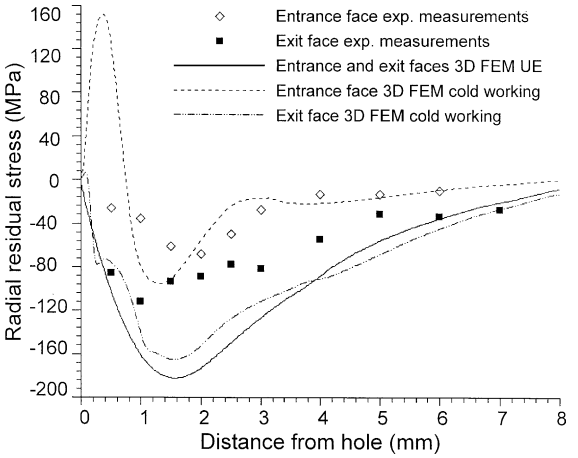

Fig. 10. Radial residual stress, for $\theta = 0°$, hardening material behaviour.

Figs. 12 and 13 compares the experimental X-ray measurements with FEA results considering an MEPP material model, for $\theta = 90°$. Figs. 14 and 15 compares the experimental X-ray measurements with FEA results considering an hardening material behaviour, for $\theta = 90°$.

FEA results are somewhat different from the experimental measurements. It was noticed that on the entrance face FEA results have the same

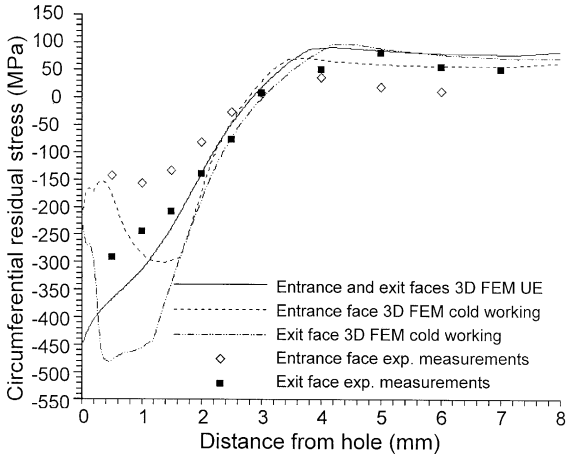

Fig. 11. Circumferential residual stress, for $\theta = 0°$, hardening material behaviour.

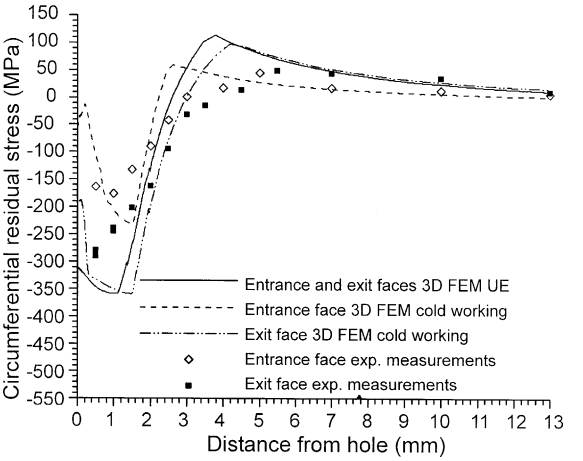

Fig. 13. Circumferential residual stress, for $\theta = 90°$, MEPP.

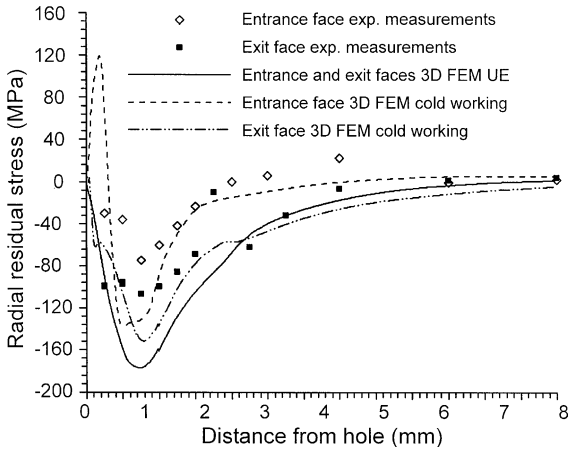

Fig. 12. Radial residual stress, for $\theta = 90°$, MEPP.

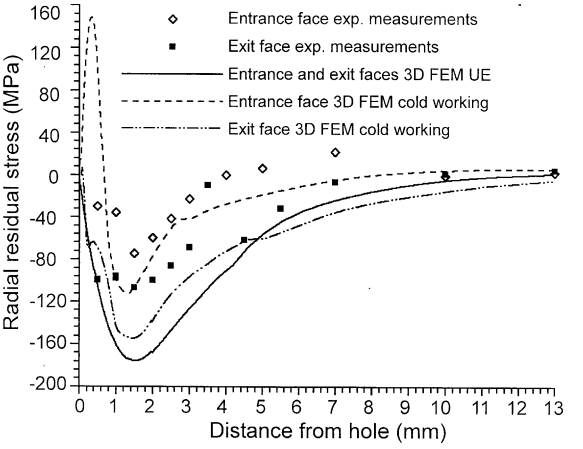

Fig. 14. Radial residual stress, for $\theta = 90°$, hardening material behaviour.

trend as the corresponding experimental measurements. The same thing happens for the exit face. Larger differences were found for the hardening material behaviour because higher residual stress values were found elsewhere. Along $\theta = 90°$ the agreement between both types of results is better. This better agreement can be due to the larger number of experimental measurements, taken along a larger specimen length.

In both situations $\theta = 0°$ and $\theta = 90°$ close to the hole the agreement is poor because experimental measurements are averaged over an irradiated volume, and it is not possible to resolve the steep stress gradients in the vicinity of the hole, Ref. [24].

5. Fatigue striation spacing measurements

The specimens' geometry is a rectangular plate (280 mm × 25 mm) with a central hole of 4.83 mm diameter. Two specimens one with and other

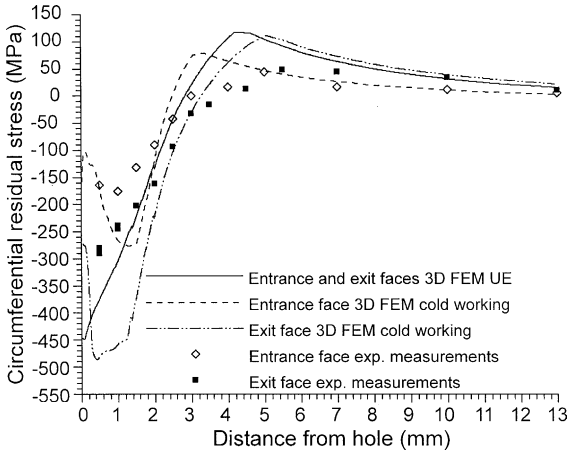

Fig. 15. Circumferential residual stress, for $\theta = 90°$, hardening material behaviour.

without residual stress were fatigue tested at a constant maximum stress level of 140 MPa, at stress ratio $R = 0.1$ and frequency $f = 10$ Hz in order to study the residual stress effect on the fatigue striation spacing. Fatigue striation spacing measurements were performed using SEM. Fig. 16 presents one of the crack surfaces observed. As an example the striations observed for a given crack length are presented in Fig. 17 for both specimens. Fig. 18 shows that for equal fatigue loading conditions striation spacing is lower for the cold-worked specimen, along the crack surface.

6. Conclusions

1. Using the experimental X-ray technique inevitably the stresses are averaged over the irradiated volume. Therefore it is not possible to resolve the steep stress gradients in the vicinity of the hole, and the peak values predicted by finite element simulation result underestimated.
2. The cold-working finite element simulations presented seem to be in general agreement with experimental results.

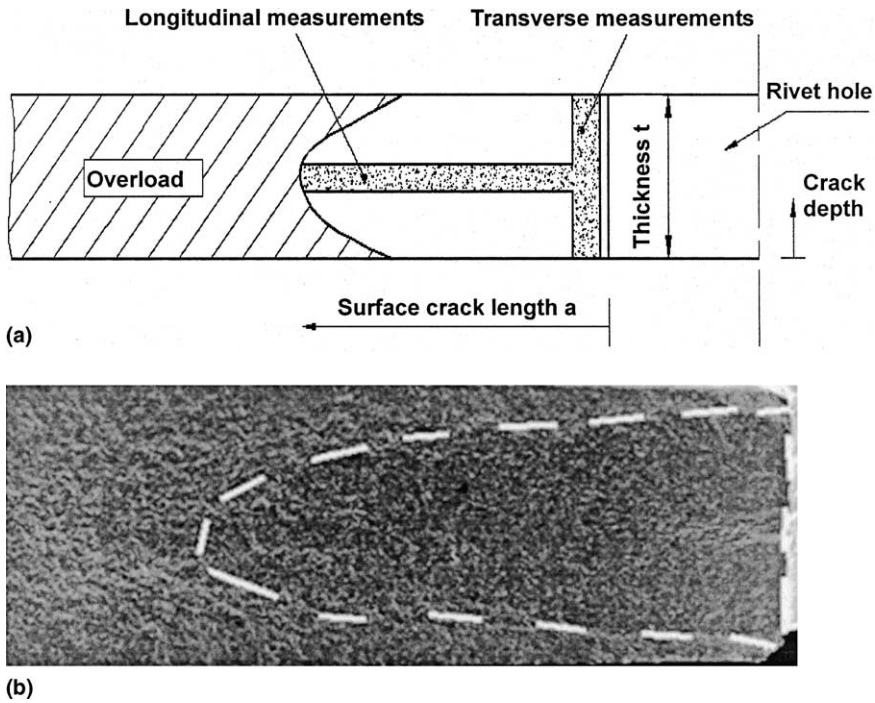

Fig. 16. (a) Schematic representation of the longitudinal and transverse direction of measurements; (b) fatigue crack, left side.

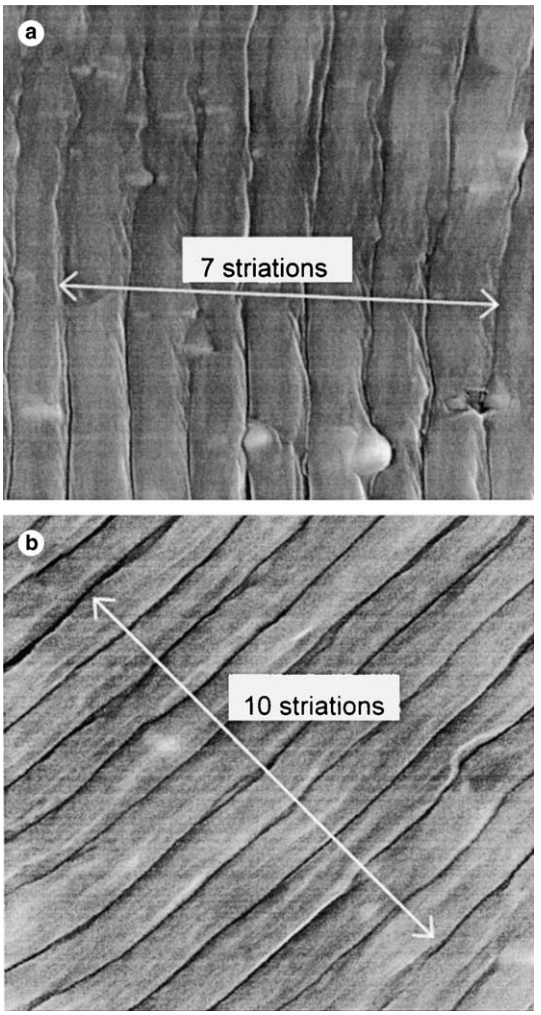

Fig. 17. Fatigue striation spacing: (a) Normal hole, crack length $a = 2.71$ mm (×20,000); (b) cold-worked, crack length $a = 2.50$ mm (×40,000).

3. Fatigue striation spacing measurements along the crack length for two open hole specimens with and without residual stress were presented. Fatigue striation spacing along the crack length decrease due to the residual stress effect. As it is known striations spacing can be directly related with the crack growth process.
4. The specimens' fatigue lives were 200224 and 70986 cycles for cold-worked and normal hole specimen, respectively. In the present work the crack growth rate decreasing due to cold-working was traduced by a longer fatigue life.

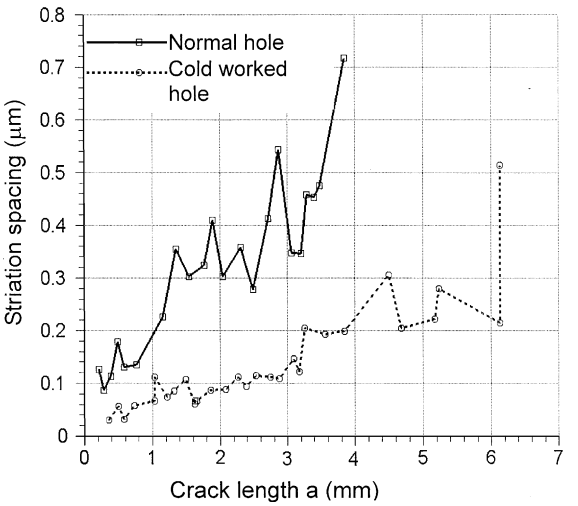

Fig. 18. Mean striation spacing along the crack length a, in both specimens.

Acknowledgments

The present work is part of the IDMEC contribution for the ADMIRE project (contract G4RD-CT-2000-0396) of the European Union. The X-ray measurements were performed in the frame of the POCTI/33681/CTM 2000 project of Portuguese Foundation for the Science and Technology (FCT) sponsored by the European Regional Development Fund. Specimens were provided by DASA-Hamburg. The SEM work of Ms Daniela Silva (CEMUP) is acknowledged.

References

[1] G. Clark, Modeling residual-stresses and fatigue crack-growth at cold-expanded fastener holes, Fatigue and Fracture of Engineering Materials and Structures 14 (5) (1991) 579–589.
[2] J. Kang, W.S. Johnson, D.A. Clark, Three-dimensional finite element analysis of the cold expansion of fastner holes in two aluminium alloys, Journal of Engineering Materials and Technology 124 (2002) 140–145.
[3] D.L. Ball, Elastic–plastic stress-analysis of cold expanded fastener holes, Fatigue and Fracture of Engineering Materials and Structures 18 (1) (1995) 47–63.
[4] C. Poussard, M.J. Pavier, D.J. Smith, Analytical and finite element predictions of residual stress in cold-worked fastner holes, Journal of Strain Analysis 30 (4) (1995) 291–304.

[5] G. Wanlin, Elastic–plastic analysis of finite sheet with a cold worked hole, Engineering Fracture Mechanics 45 (6) (1993) 857–864.
[6] G.A. Webster, A.N. Ezeilo, Residual stress and their influence on fatigue lifetimes, International Journal of Fatigue 23 (2001) S375–S383.
[7] M. Priest et al., An assessment of residual stress measurements around cold-worked holes, Experimental Mechanics (1995) 361–366.
[8] D.L. Ball, D.R. Lowry, Experimental investigation on the effects of cold expansion of fastener holes, Fatigue and Fracture of Engineering Materials and Structures 21 (1) (1998) 17–34.
[9] L. Schwarmann, On improving the fatigue performance of a double-shear lap joint, International Journal of Fatigue 5 (2) (1983) 105–111.
[10] A.F. Grandt Jr., Stress intensity factors for some thought-cracked fastner holes, International Journal of Fracture 5 (2) (1975) 283–294.
[11] A.F. Grandt Jr., J.P. Gallagher, Proposed fracture mechanics criteria to select mechanical fasteners for long service lives, in: Fracture Toughness and Slow-stable Cracking, ASTM STP, 1974, p. 559.
[12] R.A. Pell et al., Fatigue of thick-section cold-expanded holes with and without cracks, Fatigue and Fracture of Engineering Materials and Structures 12 (6) (1989) 553–567.
[13] M. Bernard, T. Bui-Quoc, M. Burlat, Effect of re-cold-working on fatigue life enhancement of a fastner hole, Fatigue and Fracture of Engineering Materials and Structures 8 (7/8) (1995) 765–775.
[14] P. Papanikos, Mechanics of Mixed Mode Fatigue Behaviour of Cold Worked Adjacent Holes, University of Toronto, 1997.
[15] M.J. Pavier, C.G.C. Ponssard, D.J. Smith, Finite element modelling of the interaction of residual stress with mechanical load for a crack emanating from a cold worked fastener hole, Journal of Strain Analysis for Engineering Design 33 (4) (1998) 275–289.
[16] A. Leon, Benefits of split mandrel cold working, International Journal of Fatigue 20 (1) (1998) 1–8.
[17] J. Schijve, Fatigue of Structures and Materials, Kluwer Academic Publishers, The Netherlands, 2001.
[18] J.P. Pina et al., Residual stresses and crystallographic texture in hard chromium electroplated coatings, Surface and Coatings Technology 96 (1997) 148–162.
[19] ABAQUS User's Manual, Hibbitt, Karlsson and Sorenson, Pawtucket, RI, 2001.
[20] M.J. Pavier, C.G.C. Poussard, D.J. Smith, A finite element simulation of the cold working process for fastener holes, Journal of Strain Analysis for Engineering Design 32 (4) (1997) 287–300.
[21] M.J. Pavier, C.G.C. Poussard, D.J. Smith, Effect of residual stress around cold worked holes on fracture under superimposed mechanical load, Engineering Fracture Mechanics 63 (6) (1999) 751–773.
[22] E.W. O'Brien, Beneficial residual stress from the cold expansion of large holes in thick light alloy plate, Journal of Strain Analysis for Engineering Design 35 (4) (2000) 261–276.
[23] FTI, Cold Expansion Holes Using the Standard Split Sleeve System and Countersink Cole Expansion, Fatigue Technology Inc., Andover Park West, Seatle, Washington, USA, 2002.
[24] R. Cook, P. Holdway, Residual stress induced by hole cold expansion, in: First International on Computer Methods and Experimental Measurements for Surface Treatment Effects, Computational Mechanics Publications, 1993.